Title

IL-36 Induces Bisphosphonate-Related Osteonecrosis of the Jaw-Like Lesions in Mice by Inhibiting TGF-β-Mediated Collagen Expression

Journal

Journal of Bone and Mineral Research, 32(2)

ISSN

0884-0431

Authors

Kim, Sol
Williams, Drake W
Lee, Cindy
et al.

Publication Date

2017-02-01

DOI

10.1002/jbmr.2985

Peer reviewed

HHS Public Access

Author manuscript

J Bone Miner Res. Author manuscript; available in PMC 2018 February 01.

Published in final edited form as:

J Bone Miner Res. 2017 February ; 32(2): 309–318. doi:10.1002/jbmr.2985.

IL-36 Induces Bisphosphonate-Related Osteonecrosis of the Jaw-Like Lesions in Mice by Inhibiting TGF-β-Mediated Collagen Expression

Sol Kim[1,*], **Drake W Williams**[1,*], **Cindy Lee**[1], **Terresa Kim**[1], **Atsushi Arai**[1], **Songtao Shi**[2], **Xinmin Li**[3], **Ki-Hyuk Shin**[1,4], **Mo K Kang**[1,4], **No-Hee Park**[1,3,4], and **Reuben H Kim**[1,4]

[1]The Shapiro Family Laboratory of Viral Oncology and Aging Research, UCLA School of Dentistry, Los Angeles, CA, USA

[2]Department of Anatomy and Cell Biology, University of Pennsylvania, School of Medicine, Philadelphia, PA, USA

[3]Department of Medicine, David Geffen School of Medicine at UCLA, Los Angeles, CA, USA

[4]UCLA Jonsson Comprehensive Cancer Center, Los Angeles, CA, USA

Abstract

Long-term administration of nitrogen-containing bisphosphonates can induce detrimental side effects such as bisphosphonate-related osteonecrosis of the jaw (BRONJ) in human. Although inflammation is known to be associated with BRONJ development, the detailed underlying mechanism remains unknown. Here, we report that the pro-inflammatory cytokine IL-36α is, in part, responsible for the BRONJ development. We found a notably higher level of IL-36α and lower level of collagen in the BRONJ lesions in mice. We also found that IL-36α remarkably suppressed TGF-β-mediated expression of *Colla1* and *α-Sma* via the activation of Erk signaling pathway in mouse gingival mesenchymal stem cells. When IL-36 signaling was abrogated in vivo, development of BRONJ lesions was ameliorated in mice. Taken together, we showed the pathologic role of IL-36α in BRONJ development by inhibiting collagen expression and demonstrated that IL-36α could be a potential marker and a therapeutic target for the prevention and treatment of BRONJ.

Keywords

IL-36; OSTEONECROSIS OF THE JAW; BISPHOSPHONATE; COLLAGEN; TGF-β; Erk

Address correspondence to: Reuben H Kim, DDS, PhD, UCLA School of Dentistry, Center for the Health Sciences, Room 43-009, 10833 Le Conte Avenue, Los Angeles, CA 90095, USA. rkim@dentistry.ucla.edu.

*SK and DWW contributed equally to this work.

Additional Supporting Information may be found in the online version of this article.

Disclosures

All authors state that they have no conflicts of interest.

Introduction

Nitrogen-containing bisphosphonates (N-BPs) are anti-resorptive drugs commonly prescribed to treat bone disorders such as osteoporosis[1] or bone metastasis in cancer patients.[2] Long-term users of these drugs are at a higher risk of developing bisphosphonate-related osteonecrosis of the jaw (BRONJ), a rare but detrimental side effect that specifically occurs in the oral cavity. A recent position paper reported by the American Association of Oral and Maxillofacial Surgeons (AAOMS) redefined the definition of BRONJ to mediation-related ONJ (MRONJ) to be more inclusive of other medications that are associated with ONJ, such as denosumab or bevacizumab.[3] MRONJ is clinically defined as exposed necrotic bone with incomplete oral mucosal closure for at least 8 weeks without history of radiation exposure to the head and neck. Although the first report of ONJ induced by N-BPs was published in 2003,[4] the exact pathophysiology of ONJ development is still largely unknown.

Currently, several risk factors are known to be associated with ONJ development. Among them, dental-related trauma such as a tooth extraction is one of the major risk factors significantly associated with ONJ development in N-BP or Dmab users.[5] In clinics, a tooth extraction procedure is usually performed because of underlying pathological conditions such as severe periodontitis or periapical endodontic lesions, which cause destruction to the surrounding environment should the affected tooth remain unextracted. Indeed, preexisting pathological inflammatory conditions such as periodontal or periapical diseases are also known to be risk factors for ONJ development.[5,6] As such, these clinical observations suggest that, in addition to tooth extraction, certain inflammatory cues may be associated with ONJ development.

IL-36 family genes are relatively new members of the interleukin-1 (IL-1) family that were identified based on their sequence similarity to IL-1α and IL-1β.[7] Originally named as IL-1F6, IL-1F8, and IL-1F9, their designations were changed to IL-36α, IL-36β, and IL-36γ, respectively, because of their similarity in functions.[8] All three IL-36 members elicit signaling through IL-1 receptor-related protein 2 (IL-1Rrp2) and IL-1 receptor accessory protein (IL-1RAcP)—two subunits that make up the IL-36 receptor—and activate pathways such as NF-κB, p38, or Erk.[9,10] Increasing lines of evidence support a notion that IL-36 is implicated in inflammation-related human diseases such as psoriasis, alopecia, brain micromotion, obesity, joint disease, and allergen-induced lung inflammation.[11] However, whether IL-36 has any pathologic roles in ONJ development is yet to be determined.

Previously, we showed that both N-BP and Dmab induced ONJ-like lesions in mice.[12] Although the mechanisms of actions for N-BP and Dmab are clearly different,[13] our study and clinical findings suggest that both drugs can induce ONJ development.[3,12] Therefore, in this study, we specifically focused on examining the underlying mechanisms of ONJ development by bisphosphonates. To better understand the mechanisms by which BRONJ develops at the molecular level, we performed a microarray analysis using osteomucosal tissues obtained from tooth-extracted sites in BP- or vehicle (Veh)-treated mice and explored differentially regulated genes in vivo. Here, we identified pro-inflammatory cytokine IL-36α as one of the genes highly upregulated in ONJ lesions and demonstrated that IL-36α plays

an etiological role in BRONJ development. We also provide mechanistic evidence that there is a cross-talk between the IL-36 and TGF-β signaling pathways, leading to inhibition of collagen expression. Finally, we show that abrogation of the IL-36α signaling pathway significantly ameliorates BRONJ development in mice.

Materials and Methods

Reagents and antibodies

The following reagents were used: Erk inhibitor, U0126 (Sigma-Aldrich, St. Louis, MO, USA); ZOL (LKT Laboratories, St. Paul, MN, USA), and Zometa (Novartis Oncology, East Hanover, NJ, USA). Recombinant IL-36α (7059-ML), IL-36β (7060-ML), IL-36γ (6996-ML), and TGF-β (7666-MB) were obtained from R&D Systems (Minneapolis, MN, USA). The following antibodies were used: mouse anti-IL-36α from R&D Systems; mouse anti-α-Sma and mouse anti-α-tubulin from Sigma-Aldrich; rabbit anti-p-Smad2, mouse anti-Smad2, rabbit anti-p-IκBα, rabbit anti-IκBα, rabbit anti-p-p38, rabbit anti-p38, rabbit anti-p-p65, rabbit anti-p-Erk 1/2, and rabbit anti-Erk 1/2 from Cell Signaling Technology (Danvers, MA, USA); mouse anti-p65 from Millipore (Chicago, IL, USA); and rabbit anti-Col1a1, rabbit anti-lamin B1, and mouse anti-Gapdh from Santa Cruz Biotechnology (Dallas, TX, USA). IL-1Rrp2 neutralizing antibody used in the mice study was obtained from Amgen (Thousand Oaks, CA, USA).

Cells and cell culture

Primary gingival mesenchymal stem cells (GMSCs) were isolated from the mouse's palatal tissues as described previously.[14] Briefly, palatal tissues from C57BL/6 mice were excised and minced into small pieces, which were then subjected to collagen digestion in 37°C for 2 hours with constant agitation. Digested tissues were then collected, washed, and plated onto the culture dish containing α-MEM (Life Technologies, Carlsbad, CA, USA), 20% FBS (Life Technologies), glutamine (200 mM; Life Technologies), and 2-mercaptoethanol (55 mM; Sigma-Aldrich). From this primary culture, multi-colonies were obtained and maintained. GMSCs that are under 5 passages were used. To knockdown expression of *IL-1Rrp2*, we transfected *IL-1Rrp2* siRNA (Santa Cruz) using Lipofectamine RNAimax (Life Technologies) for 12 hours. IL-36α was then added for additional 2 days, and the cells were harvested for qRT-PCR analysis. All experiments using mice in this study were performed according to the approved institutional guidelines from the Chancellor's Animal Research Committee (ARC # 2011-062).

Animals

Eight-week-old female C57BL/6 mice were purchased from the Jackson Laboratory (Bar Harbor, ME, USA) and *IL-1Rrp2* KO mice were obtained from Taconic Bioscience (Hudson, NY, USA). All mice were kept in a pathogen-free vivarium in the UCLA Division of Laboratory Animal Medicine (DLAM) according to the approved institutional guidelines from the Chancellor's Animal Research Committee (#2011-062). The mouse model for BRONJ used in this study is previously described.[12] Briefly, ZOL (Zometa, 125 μg/kg; Novartis Oncology) or vehicle (Veh) solution (0.9% NaCl saline) was intravenously administered biweekly throughout the experiment (n = 5–10 per group). One week after

ZOL administration, maxillary first molar was extracted and allowed to heal. After 2 weeks, maxillae were harvested, and osteomucosal tissues at the tooth-extracted sites were excised and subjected to further analysis for microarray. For BRONJ-rescue experiments, anti-IL-1Rrp2 neutralizing antibody was administered 1 week before ZOL administration. One week after ZOL administration, maxillary first molar was extracted, mice were allowed to heal for 3 weeks, and the maxillae were harvested for further analysis.

cDNA microarray

Gene expression profiling was performed using the Affymetrix GeneChip Mouse 430 2.0 Array (Affymetrix, Santa Clara, CA, USA). Total RNA was extracted from osteomucosal samples of BRONJ-like lesions using the RNeasy Mini Kit (Qiagen, Valencia, CA, USA) according to the manufacturer's instruction. RNA integrity was evaluated using an Agilent 2100 Bioanalyzer (Agilent Technologies, Palo Alto, CA, USA), and purity/concentration was determined using a NanoDrop 8000 (NanoDrop Products, Wilmington, DE, USA). Microarray experiments were performed at UCLA CMC. Microarray targets were prepared using NuGEN WT-Ovation Formalin-Fixed Paraffin-Embedded RNA Amplification System and FL-Ovation cDNA Biotin Module V2 (NuGEN Technologies, San Carlos, CA, USA) and then hybridized to the array, all according to the manufacturer's instructions. The arrays were washed and stained with streptavidin phycoerythrin in Affymetrix Fluidics Station 450 using the Affymetrix GeneChip protocol and then scanned using an Affymetrix GeneChip Scanner 3000. The acquisition and initial quantification of array images were conducted using the AGCC software (Affymetrix). The subsequent data analyses were performed using Partek Genomics Suite Version 6.4 (Partek, St. Louis, MO, USA). Differentially expressed genes were selected at ≥2-fold and $p < 0.005$.

Micro-computed tomography (μCT) scan and three-dimensional volumetric analysis

The harvested maxillae were fixed with 4% paraformaldehyde in PBS, pH 7.4, at 4°C overnight and stored in 70% ethanol solution. The fixed maxillae were subjected to μCT scanning (Scanco μCT 40, Scanco Medical, Brüttisellen, Switzerland) using a voxel size of 20 μm^3 and a 0.5 mm aluminum filter. Two-dimensional slices from each maxilla were combined using μCT v6.1 software (Scanco Medical) to form a three-dimensional reconstruction. Reconstructions were further analyzed so that the viewing angles could provide an accurate representation of bone resorption after 3 weeks of healing. The scanning and analyses of data abide by the published guidelines for assessing bone microstructure in rodents.[15]

Histomorphometric analysis

After μCT scanning, these tissues were decalcified with 5% EDTA and 4% sucrose in PBS (pH 7.4). Decalcification continued for 2 to 3 weeks at 4°C. The decalcification solution was changed daily. Tissue samples were sent to the UCLA Translational Procurement Core Laboratory (TPCL) and processed for paraffin embedding.

Amounts of empty lacunae and necrotic bone percentages were evaluated as described previously.[12] Briefly, four sections (#1, #6, #11, and #16) per sample in 5 μm thickness were stained with H&E. For each section that contains an area of interest covering first

molar extracted sites horizontally from the buccal plates toward the palatal suture (~1.4 mm) and vertically from the tip of the extracted site to the bottom of the palatal bone (~0.8mm), the digital images of each section were obtained using the microscope (Olympus, DP72) at 100×. The percentage of necrotic bone was defined as an area that contains five or more empty lacunae per 1 mm^2 divided by total bone areas. The number of empty lacunae was also evaluated per total bone area (#/mm^2). The total bone surface area was measured using ImageJ software.

Immunohistochemical (IHC) staining

IL-36 expression was determined as described previously.[16] Briefly, slides were deparaffinized at 60°C in oven for 30 minutes followed by rehydration in xylene and ethanol. The slides were then unmasked in citrate buffer (6 mM citric acid/34 mM sodium citrate/pH.6.0) above 95°C for 25 minutes, and the endogenous peroxidase were blocked with 3% hydrogen peroxide (H_2O_2). The slides were incubated with 10% blocking buffer for 30 minutes, anti-IL-36 antibody or anti-mouse IgG (Vector Laboratories, Burlingame, CA, USA) antibodies (1:100) in 3% blocking buffer for 90 minutes, secondary antibody (1:200) in 3% blocking buffer for 60 minutes, and HRP-Avidin (1:1000) in PBST for 30 minutes. The slides were developed using DAB substrate kit (Vector Laboratories).

RNA isolation and real-time quantitative RT-PCR (qRT-PCR)

Total RNA was isolated from the cultured cells using RNeasy Plus Mini Kit (Qiagen). DNA-free total RNA (5 μg) was dissolved in 15 μL DEPC-H_2O, and the RT reaction was performed in first-strand buffer (Invitrogen) containing 300U Superscript II (Invitrogen), 10 mM DTT, 0.5 μg random hexamer (Promega Corporation, Madison, WI, USA), and 125 μM dNTPs. The annealing reaction was carried out for 5 minutes at 65°C, and cDNA synthesis was performed for 2 hours at 37°C, followed by incubation for 15 minutes at 70°C to stop the enzyme reaction. The RT product was diluted with 70 μl H_2O. The primers used for PCR amplification are listed in Supplemental Table S1.

Nuclear and cytoplasmic proteins fractionation

Cells were pretreated with IL-36 α for 6 hours and then treated with TGF-β1 for 2 hours. After cells were harvested, nuclear and cytoplasmic proteins were isolated using the NE-PER Nuclear and Cytoplasmic Extraction Reagents Kit (Pierce, Rockford, IL, USA) following the manufacturer's instructions.

Western blotting

Cells were washed twice with PBS before treatment with ice-cold lysis buffer (20 mM Tris-HCl, pH 7.4, 150 mM NaCl, 5 mM EDTA and 1% Triton X-100). And then, the cells were scraped and incubated on ice for 10 minutes. Cell debris was separated by centrifugation at 20,000*g* at 4°C for 20 minutes and the supernatant was collected for Western blot analysis after 8% or 10% SDS-PAGE. After electrophoresis, proteins were transferred to immobilized membrane (Millipore), which was subsequently blocked with 5% non-fat milk for 1 hour at room temperature. Then, membrane was incubated with primary antibodies,

and probed with the respective secondary antibodies conjugated with HRP. The signals were obtained using ChemiDoc XRS System (Bio-Rad, Hercules, CA, USA).

ELISA

Sera collected from each mouse was stored in −20°C and thawed once. The presence of TRAP-5b was detected by sandwich ELISA using the MouseTRAP Kit (Immunodiagnostic Systems, Fountain Hills, AZ, USA). Systemic levels of IL-36α were detected by sandwich ELISA established in our laboratory using IL-36α and biotinylated IL-36α antibodies (AF2297 and BAF2297; R&D Systems). Soluble collagens were detected according to manufacturer's protocol using the Sircol assay kit (QZBCOL1-1; Cedarlane Laboratories, Burlington, NC, USA).

Chromatin immunoprecipitation (ChIP) assay

Cells were fixed at room temperature for 10 minutes in the culture medium containing 1% formaldehyde, and ChIP assay was performed using the MAGnify ChIP System (Invitrogen) according to the manufacturer's instructions. Col1a1 and α-Sma antibodies were coupled to Dynabeads, and the antibody-coupled Dynabeads were incubated with the sheared chromatin. Chromatin-antibody-Dynabeads complexes were then washed with washing buffers, and the cross-links were reversed in the presence of Proteinase K. The uncross-linked DNA was purified using the DNA Purification Magnetic Beads. The purified DNA fragments were amplified using primer sets. These primers are listed in Supplemental Table S2.

Statistical analysis

The outcome measurements were expressed as means ± standard deviation. To compare the outcome mean measurements among the different groups, we used one-way ANOVA with Tukey's post hoc test. For comparison between two groups, Student's *t* test was used. All statistical tests were performed using the SPSS 23 software (IBM, Somers, NY, USA). Any *p* values <0.05 are considered significant.

Results

Microarray gene profiling identifies overexpressed IL-36 family members in ONJ-like lesions in mice

Previously, we demonstrated that BP administration followed by tooth extraction induced ONJ-like lesions in mice.[12] To further gain molecular insights, we utilized a high-throughput micro-array screening system and compared differentially expressing genes in tissues obtained from ONJ lesions (Fig. 1*A*). Consistent with our previous report,[12] tooth-extracted sockets were filled in with new bone in the Veh-treated groups but remained unfilled in ZOL-treated groups (Fig. 1*B*). These unhealed osteomucosal tissues at the tooth-extracted sites were subjected to microarray profiling, and differentially expressed genes that were either upregulated or downregulated more than fivefold were obtained (Fig. 1*C*, Supplemental Table S3). When these genes were further analyzed using the ingenuity pathway analysis (IPA), we identified "biosynthesis of steroids" as the most significantly associated functional pathway (Fig. 1*D*). The primary target of N-BPs is farnesyl

diphosphate synthase (FDPS), the branch-point enzyme in the mevalonate pathway partly responsible for steroid synthesis.[17] Interestingly, genes involved in this pathway such as FDPS were all upregulated (Fig. 1*E*), presumably because of compensatory mechanisms of directly blocking the mevalonate pathway by N-BP,[18] demonstrating the validity of our BRONJ mouse model. The second functional pathway that is associated with ONJ lesions was "role of osteoblasts, osteoclasts, and chondrocytes in rheumatoid arthritis" (Fig. 1*D*). Among these genes, expression of IL-1 family cytokines IL-1F4 (IL-18), IL-1F5 (IL-36RN), IL-1F6 (IL-36α), and IL-1F8 (IL-36β) were highly upregulated (Fig. 1*F*). Because IL-36 family members were all significantly upregulated, we further analyzed the role of these genes and their possible involvement in ONJ development.

IL-36 is overexpressed in BRONJ-like lesions in mice

To confirm the microarray results, we first validated expression of IL-36 in BRONJ lesions. Consistent with the microarray data, we found increased expression of *IL-18*, *IL-36α*, *IL-36β*, and *FDPS*, but not *IL-36γ*, in a BRONJ-specific manner (Fig. 1*G, K*). Immunohistochemical analysis against IL-36α and IL-18 showed high levels of both IL-36α and IL-18 at the leading edge of epithelia near the wounded site in BRONJ but not in Veh-treated mice (Fig. 1*L*). The serum level of IL-36α, but not IL-18, in ZOL-treated mice was also significantly elevated when compared with the Veh-treated mice (Fig. 1*M, N*). Collectively, these data suggest that IL-36α is upregulated both locally and systemically in mice with BRONJ-like lesions.

IL-36 inhibits TGF-β-mediated collagen expression in GMSCs

One of the hallmarks in the BRONJ lesions in patients is denuded bone with a lack of covering collagen-enriched connective tissue layers.[3] In gingival connective tissue, type I collagen (Col1a1) is the major constituent.[19] Further analysis from the microarray data revealed that many genes associated with connective tissues (ie, collagenous and non-collagenous proteins) including *Col1a1* were significantly downregulated in BRONJ-like lesions (Fig. 2*A*). Collagen is an essential protein in proper wound healing, and dysregulation of collagen deposition by fibroblasts leads to impaired wound healing.[20] Thus, we examined whether IL-36 plays any role in suppressing collagen expression. When we treated gingival mesenchymal stem cells (GMSCs) with recombinant IL-36α, IL-36β, or IL-36γ, there was significant induction of *IL-6* expression (Fig. 2*B*), a known target of IL-36.[21] When we examined expression of *Col1a1*, *Col1a2*, and *Col3a1*, they were all suppressed at the mRNA level (Fig. 2*C*). Knockdown of IL-1Rrp2 rescued suppressed collagen expression of *Col1a1* and *Col1a2* but not *Col3a1*, suggesting that IL-36 may mediate the expression of *Col3a1* differently from that of *Col1a1* and *Col1a2* (Fig. 2*D, E*). Interestingly, IL-36 treatment did not show any drastic effects at the protein expression level, presumably because of low basal collagen expression (Fig. 2*F*, left two panels). Because TGF-β is known to play an important role in wound healing by controlling collagen synthesis,[22] we tested whether IL-36α suppresses TGF-β-mediated collagen expression. Indeed, TGF-β significantly induced protein levels of Col1a1 as well as α-Sma, which is required for wound contraction,[23] but such induction was suppressed by IL-36α treatment (Fig. 2*F*, right two panels). Secreted collagen was also suppressed by IL-36α treatment (Fig.

2*G*). Similar results were noted at the mRNA level, suggesting that IL-36α suppresses TGF-β-mediated expression of *Col1a1*, *Col1a2*, and *α-Sma* at the transcriptional level (Fig. 2*H*).

IL-36α inhibits TGF-β-mediated nuclear translocation of the Smad complex by activating the Erk signaling pathway

To further gain molecular insights as to how IL-36α suppresses TGF-β-mediated collagen expression, we examined whether Smad signaling is altered by IL-36α. When phosphorylated Smad2 (p-Smad2) was screened in the whole cell lysate of GMSCs treated with TGF-β and different doses of IL-36α, we found no differences in p-Smad2 level (Fig. 3*A*). However, there was a significant reduction of p-Smad2 in the nuclear fractions in a dose-dependent manner (Fig. 3*B*), whereas p-Smad2 level in the cytoplasmic fractions was not affected (Fig. 3*C*), indicating that IL-36α inhibited TGF-β-activated nuclear translocation of the Smad complex. Consistent with this finding, the occupancy of Smad2 in the *Col1a1* and *α-Sma* promoters by TGF-β was significantly reduced by IL-36α (Fig. 3*D, E*).

IL-36 is known to activate several intracellular signaling pathways including NF-κB, p38, and Erk.[24] In particular, activation of the NF-κB signaling pathway by IL-36α has been previously shown.[10] To investigate which intra-signaling pathway is responsible for IL-36α-mediated suppression of collagen expression by TGF-β in GMSCs, we treated GMSCs with different doses of IL-36α and screened for activation of these pathways. IL-36 activated both NF-κB and MAPK signaling pathways as determined by induced phosphorylation of p65 and Erk1/2 (Fig. 3*F*). Interestingly, there was no phosphorylation of IκBα, a required step for its own degradation, which in turns allows for nuclear translocation of NF-κB complex,[25] suggesting that effects of IL-36α on the NF-κB signaling pathway may be dispensable. Indeed, a recent study demonstrated that IL-36α does not have any effects on osteoclast formation in which the NF-κB signaling pathway is known to play a critical functional role.[26] On the other hand, there was a notable increase in p-Erk 1/2 (Fig. 3*F*). When the Erk signaling pathway was inhibited by the Erk-specific inhibitor, U0126, IL-36α-mediated suppression of *Col1a1* and *α-Sma* expression was rescued (Fig. 3*G, H*). Furthermore, U0126 rescued IL-36α-mediated inhibition of p-Smad2 nuclear translocation in TGF-β-treated GMSCs (Fig. 3*I, J*), indicating that the activation of Erk1/2 has a predominant and functional role in IL-36α-treated GMSCs. Our study is consistent with the previous finding that activation of Erk1/2 signaling pathway disrupts TGF-β1-stimulated Smad2/3 nuclear translocation.[27] When GMSCs obtained from *Rrp2*$^{-/-}$ mice were treated with IL-36α, suppression of TGF-β-mediated p-Smad2 was also abolished in nuclear but not cytoplasmic fractions (Fig. 3*K–N*), further confirming that activation of the IL-36 signaling pathway via the IL-36 receptor is required for inhibition of TGF-β-activated nuclear translocation of the Smad complex. These data indicate that IL-36α inhibits TGF-β-activated nuclear translocation of the Smad complex by activating the Erk signaling pathway.

The IL-1Rrp2 neutralizing antibody rescues BRONJ-like lesions in mice

We next examined whether blocking the IL-36 signaling pathway by targeting the IL-36 receptor, IL-1Rrp2, would rescue BRONJ lesions in mice. When IL-1Rrp2 was knocked

down in GMSCs, collagen expression suppressed by IL-36α was rescued in vitro (Fig. 2*D, E*). To block the IL-36 signaling pathway in vivo, we used an anti-IL-1Rrp2 neutralizing antibody (Fig. 4*A*). Administration of the anti-IL-1Rrp2 neutralizing antibody itself did not alter any effects of bisphosphonates in vivo as demonstrated by circulating tartrate-resistant acid phosphatase (TRAP) 5b (Fig. 4*B*), an indicator of activated osteoclast number.[28] When mice were harvested, we found that 20% of the mice treated with ZOL alone had exposed bone, results of which is consistent with previous findings,[12,29] indicating breached oral mucosal tissues and unfilled tooth-extracted sockets, respectively (Fig. 4*C, D*, third row). In contrast, no exposed bone was found in any of the other test groups, including ZOL in combination with anti-IL-1Rrp2 neutralizing antibody (Fig. 4*C, D*). Histological examination revealed an absence of connective tissues on the exposed bone area in the ZOL-treated group, whereas complete oral mucosal closures were noted in the other groups (Fig. 4*E*). Further analysis showed that empty lacunae and necrotic bone was significantly rescued in the presence of anti-IL-1Rrp2 neutralizing antibody (Fig. 4*F, G*), indicating that blocking the IL-36 signaling pathway ameliorated BRONJ lesions in mice.

Discussion

In this study, we showed that the pro-inflammatory cytokine IL-36 is a putative molecular determinant in BRONJ development by providing compelling evidence at the molecular, cellular, and organismal levels. We also demonstrated a novel cross-talk between IL-36 and TGF-β; IL-36 activates the Erk signaling pathway, which inhibits TGF-β-activated nuclear translocation of the Smad complex (Figs. 2, 3, and 5). To the best of our knowledge, our study is the first report demonstrating the involvement of IL-36 in BRONJ development, adding another pathologic role of IL-36 to the growing list of the IL-36-mediated human diseases and shedding new insights as to how ONJ develops, at least by N-BPs.

IL-36 is implicated in inflammation-related human diseases by targeting immune cells.[30] Interestingly, a recent study suggested that IL-36 can also assert its effects on non-immune cells that express IL-1Rrp2; IL-36α secreted from CD138-postive plasma cells in the psoriatic and rheumatoid arthritis synovium induced expression of IL-6 and IL-8 in synovial fibroblasts.[31] Similarly, our study demonstrated that GMSCs express a high level of IL-1Rrp2 and that IL-36α significantly inhibits TGF-β-mediated expression of *Col1a1* and *α-Sma* (Figs. 2 and 3), suggesting the diverse involvement of IL-36 in pathologic lesions.

Although our study demonstrated the upregulation of IL-36 in ZOL-treated mice in an ONJ-specific manner and the suppression of collagen expression by IL-36, the source of IL-36 is yet to be determined. Studies suggest that IL-36 is predominantly expressed in keratinocytes and is known to play a role in psoriasis via its interplay with psoriasis-associated cytokines such TNF-α, IL-6, and IL-17.[11,32] Indeed, our IHC staining showed that IL-36 is heavily expressed at the migrating tongue of the epithelial cells that are specific to BRONJ lesions, suggesting IL-36 is primarily secreted by epithelial cells when the healing process (eg, wound closure) is incomplete by BPs, leading to BRONJ lesions.

On the contrary, IL-36 is also significantly produced by monocyte-lineages such as dendritic cells and macrophages.[7,33] Because osteoclasts are derived from monocyte/macrophage

lineages and are the first cells to encounter BPs when BPs are leached out from bone during resorption, it is tempting to speculate that BPs taken up by osteoclasts may cause significant release of IL-36, interfering with local collagen formation. Further studies are required to elucidate the primary sources of IL-36 that play an etiologic role in BRONJ.

Several lines of evidence from previous studies support a notion that IL-36 may play additional etiological roles in ONJ development. First, IL-36 in human keratinocytes can be induced by IL-17,[32] an important cytokine known to be associated with BRONJ.[34] Second, IL-36 is shown to be present in the gingival crevicular fluid in periodontal diseases, one of the known risk factors for ONJ development.[3,35] Third, induction of IL-36 is also observed in response to microbial or viral exposures,[36,37] and externalization of cytoplasmic IL-36 occurs when challenged by bacterial lipopolysaccharide.[38] Because bacterial infection is commonly found in ONJ lesions, in part because of their preferential adhesion to the exposed bone hydroxyapatite,[39,40] it is possible that the latter notion may result in amplification of IL-36 production at the local level and play a pathological role in ONJ lesions.

The current study is in line with our previous finding in which we demonstrated that deregulation in woven bone formation within the tooth-extracted sockets are associated with ONJ development by BPs.[12] One of the early steps in woven bone formation is collagen secretion to the extracellular matrix onto which osteoblasts start forming mineralization.[41] The TGF-β1 signaling pathway is significantly upregulated during the initial stages and mediates the wound healing.[42,43] Reduced TGF-β1 expression was observed in impaired wound healing and chronic ulcerations.[44,45] It is noteworthy that the TGF-β1 signaling pathway is significantly suppressed in BRONJ lesions at the clinical level.[46] Therefore, a possibility exists whereby inhibition of the initial osteomucosal wound healing process in the oral cavity by suppressing the TGF-β1 signaling pathway and woven bone formation may contribute to ONJ development.

Although our study demonstrated the involvement of IL-36 on ONJ development by N-BPs, the limitation of the current study is that it is not known whether IL-36 also etiologically causes ONJ development by Dmab. Our preliminary study showed that IL-36 expression is notably elevated in the DRONJ lesions in mice (unpublished data). Because Dmab completely abolishes osteoclast formation in vivo, the effects of IL-36 in DRONJ development may be indirectly associated with factors other than dysfunctional osteoclasts per se such as inflammation associated with unhealing tooth-extracted site. Such speculation is particularly plausible when both BRONJ and DRONJ lesions commonly exhibit the exposed necrotic bone without any overlaying connective tissues. The functional role of IL-36 in DRONJ development needs further clarification.

In conclusion, we have shown that IL-36 plays an etiological role in BRONJ development. Because there are no currently available therapeutic modalities for BRONJ development, utilizing IL-36 as a therapeutic target to ameliorate BRONJ lesions in patients warrants further investigation. Similarly, further study on the role of IL-36 in DRONJ development would provide additional clues whether inhibiting IL-36 signaling pathway may be therapeutically beneficial to managing MRONJ in general.

Supplementary Material

Refer to Web version on PubMed Central for supplementary material.

Acknowledgments

This study was supported by the grants from NIDCR/NIH R03DE021114, R01DE023348, Dean's Faculty Research Seed grant to RHK, and F30DE025172 to DWW. We thank Amgen for providing IL-1Rrp2 neutralizing antibody and IL-1Rrp2 knockout mice, and Dr Jennifer Towne for consulting. We also thank the UCLA TPCL for their expedited and cooperative services.

Authors' roles: RHK designed the project with additional contributions by SK, DWW, SS, KHS, MKK, and NHP. SK and DWW performed data collection with additional contributions by CL, TK, and AA. XL performed microarray data analysis. SS, KHS, MKK, NHP, and RHK performed data interpretation. SK, DWW, and RHK wrote the manuscript.

References

1. MacLean C, Newberry S, Maglione M, et al. Systematic review: comparative effectiveness of treatments to prevent fractures in men and women with low bone density or osteoporosis. Ann Intern Med. 2008; 148(3):197–213. [PubMed: 18087050]
2. Isla D, Afonso R, Bosch-Barrera J, Martinez N. Zoledronic acid in lung cancer with bone metastases: a review. Expert Rev Anticancer Ther. 2013; 13(4):421–6. [PubMed: 23560837]
3. Ruggiero SL, Dodson TB, Fantasia J, et al. American Association of Oral and Maxillofacial Surgeons position paper on medication-related osteonecrosis of the jaw—2014 update. J Oral Maxillofac Surg. 2014; 72(10):1938–56. [PubMed: 25234529]
4. Marx RE. Pamidronate (Aredia) and zoledronate (Zometa) induced avascular necrosis of the jaws: a growing epidemic. J Oral Maxillofac Surg. 2003; 61(9):1115–7. [PubMed: 12966493]
5. Vahtsevanos K, Kyrgidis A, Verrou E, et al. Longitudinal cohort study of risk factors in cancer patients of bisphosphonate-related osteonecrosis of the jaw. J Clin Oncol. 2009; 27(32):5356–62. [PubMed: 19805682]
6. Saad F, Brown JE, Van Poznak C, et al. Incidence, risk factors, and outcomes of osteonecrosis of the jaw: integrated analysis from three blinded active-controlled phase III trials in cancer patients with bone metastases. Ann Oncol. 2012; 23(5):1341–7. [PubMed: 21986094]
7. Smith DE, Renshaw BR, Ketchem RR, Kubin M, Garka KE, Sims JE. Four new members expand the interleukin-1 superfamily. J Biol Chem. 2000; 275(2):1169–75. [PubMed: 10625660]
8. Dinarello C, Arend W, Sims J, et al. IL-1 family nomenclature. Nat Immunol. 2010; 11(11):973. [PubMed: 20959797]
9. Blumberg H, Dinh H, Trueblood ES, et al. Opposing activities of two novel members of the IL-1 ligand family regulate skin inflammation. J Exp Med. 2007; 204(11):2603–14. [PubMed: 17908936]
10. Towne JE, Garka KE, Renshaw BR, Virca GD, Sims JE. Interleukin (IL)-1F6, IL-1F8, and IL-1F9 signal through IL-1Rrp2 and IL-1RAcP to activate the pathway leading to NF-kappaB and MAPKs. J Biol Chem. 2004; 279(14):13677–88. [PubMed: 14734551]
11. Towne JE, Sims JE. IL-36 in psoriasis. Curr Opin Pharmacol. 2012; 12(4):486–90. [PubMed: 22398321]
12. Williams DW, Lee C, Kim T, et al. Impaired bone resorption and woven bone formation are associated with development of osteonecrosis of the jaw-like lesions by bisphosphonate and anti-receptor activator of NF-kappaB ligand antibody in mice. Am J Pathol. 2014; 184(11):3084–93. [PubMed: 25173134]
13. Baron R, Ferrari S, Russell RG. Denosumab and bisphosphonates: different mechanisms of action and effects. Bone. 2011; 48(4):677–92. [PubMed: 21145999]
14. Zhang Q, Shi S, Liu Y, et al. Mesenchymal stem cells derived from human gingiva are capable of immunomodulatory functions and ameliorate inflammation-related tissue destruction in experimental colitis. J Immunol. 2009; 183(12):7787–98. [PubMed: 19923445]

15. Bouxsein ML, Boyd SK, Christiansen BA, Guldberg RE, Jepsen KJ, Muller R. Guidelines for assessment of bone microstructure in rodents using micro-computed tomography. J Bone Miner Res. 2010; 25(7):1468–86. [PubMed: 20533309]
16. Kim RH, Kang MK, Kim T, et al. Regulation of p53 during senescence in normal human keratinocytes. Aging Cell. 2015; 14(5):838–46. [PubMed: 26138448]
17. Luckman SP, Hughes DE, Coxon FP, Graham R, Russell G, Rogers MJ. Nitrogen-containing bisphosphonates inhibit the mevalonate pathway and prevent post-translational prenylation of GTP-binding proteins, including Ras. J Bone Miner Res. 1998; 13(4):581–9. [PubMed: 9556058]
18. Staal A, Frith JC, French MH, et al. The ability of statins to inhibit bone resorption is directly related to their inhibitory effect on HMG-CoA reductase activity. J Bone Miner Res. 2003; 18(1): 88–96. [PubMed: 12510809]
19. McCulloch CA, Bordin S. Role of fibroblast subpopulations in periodontal physiology and pathology. J Periodontal Res. 1991; 26(3 Pt 1):144–54. [PubMed: 1830616]
20. Singer AJ, Clark RA. Cutaneous wound healing. N Engl J Med. 1999; 341(10):738–46. [PubMed: 10471461]
21. Foster AM, Baliwag J, Chen CS, et al. IL-36 promotes myeloid cell infiltration, activation, and inflammatory activity in skin. J Immunol. 2014; 192(12):6053–61. [PubMed: 24829417]
22. Beanes SR, Dang C, Soo C, Ting K. Skin repair and scar formation: the central role of TGF-beta. Expert Rev Mol Med. 2003; 5(8):1–22.
23. Desmouliere A, Geinoz A, Gabbiani F, Gabbiani G. Transforming growth factor-beta 1 induces alpha-smooth muscle actin expression in granulation tissue myofibroblasts and in quiescent and growing cultured fibroblasts. J Cell Biol. 1993; 122(1):103–11. [PubMed: 8314838]
24. Dietrich D, Gabay C. Inflammation: IL-36 has proinflammatory effects in skin but not in joints. Nat Rev Rheumatol. 2014; 10(11):639–40. [PubMed: 25201385]
25. Viatour P, Merville MP, Bours V, Chariot A. Phosphorylation of NF-kappaB and IkappaB proteins: implications in cancer and inflammation. Trends Biochem Sci. 2005; 30(1):43–52. [PubMed: 15653325]
26. Derer A, Groetsch B, Harre U, et al. Blockade of IL-36 receptor signaling does not prevent from TNF-induced arthritis. PLoS One. 2014; 9(8):e101954. [PubMed: 25111378]
27. Zhang X, Min KW, Liggett J, Baek SJ. Disruption of the transforming growth factor-beta pathway by tolfenamic acid via the ERK MAP kinase pathway. Carcinogenesis. 2013; 34(12):2900–7. [PubMed: 23864386]
28. Naylor K, Eastell R. Bone turnover markers: use in osteoporosis. Nat Rev Rheumatol. 2012; 8(7): 379–89. [PubMed: 22664836]
29. Bi Y, Gao Y, Ehirchiou D, et al. Bisphosphonates cause osteonecrosis of the jaw-like disease in mice. Am J Pathol. 2010; 177(1):280–90. [PubMed: 20472893]
30. Gabay C, Towne JE. Regulation and function of interleukin-36 cytokines in homeostasis and pathological conditions. J Leukoc Biol. 2015; 97(4):645–52. [PubMed: 25673295]
31. Frey S, Derer A, Messbacher ME, et al. The novel cytokine interleukin-36alpha is expressed in psoriatic and rheumatoid arthritis synovium. Ann Rheum Dis. 2013; 72(9):1569–74. [PubMed: 23268368]
32. Carrier Y, Ma HL, Ramon HE, et al. Inter-regulation of Th17 cytokines and the IL-36 cytokines in vitro and in vivo: implications in psoriasis pathogenesis. J Invest Dermatol. 2011; 131(12):2428–37. [PubMed: 21881584]
33. Vigne S, Palmer G, Lamacchia C, et al. IL-36R ligands are potent regulators of dendritic and T cells. Blood. 2011; 118(22):5813–23. [PubMed: 21860022]
34. Kikuiri T, Kim I, Yamaza T, et al. Cell-based immunotherapy with mesenchymal stem cells cures bisphosphonate-related osteonecrosis of the jaw-like disease in mice. J Bone Miner Res. 2010; 25(7):1668–79. [PubMed: 20200952]
35. Kursunlu SF, Ozturk VO, Han B, Atmaca H, Emingil G. Gingival crevicular fluid interleukin-36beta (-1F8), interleukin-36gamma (-1F9) and interleukin-33 (-1F11) levels in different periodontal disease. Arch Oral Biol. 2015; 60(1):77–83. [PubMed: 25247780]

36. Vos JB, van Sterkenburg MA, Rabe KF, Schalkwijk J, Hiemstra PS, Datson NA. Transcriptional response of bronchial epithelial cells to Pseudomonas aeruginosa: identification of early mediators of host defense. Physiol Genomics. 2005; 21(3):324–36. [PubMed: 15701729]

37. Bochkov YA, Hanson KM, Keles S, Brockman-Schneider RA, Jarjour NN, Gern JE. Rhinovirus-induced modulation of gene expression in bronchial epithelial cells from subjects with asthma. Mucosal Immunol. 2010; 3(1):69–80. [PubMed: 19710636]

38. Martin U, Scholler J, Gurgel J, Renshaw B, Sims JE, Gabel CA. Externalization of the leaderless cytokine IL-1F6 occurs in response to lipopolysaccharide/ATP activation of transduced bone marrow macrophages. J Immunol. 2009; 183(6):4021–30. [PubMed: 19717513]

39. Kos M, Junka A, Smutnicka D, Bartoszewicz M, Kurzynowski T, Gluza K. Pamidronate enhances bacterial adhesion to bone hydroxyapatite Another puzzle in the pathology of bisphosphonate-related osteonecrosis of the jaw? J Oral Maxillofac Surg. 2013; 71(6):1010–6. [PubMed: 23489958]

40. Mawardi H, Giro G, Kajiya M, et al. A role of oral bacteria in bisphosphonate-induced osteonecrosis of the jaw. J Dent Res. 2011; 90(11):1339–45. [PubMed: 21921248]

41. Del Fattore A, Teti A, Rucci N. Bone cells and the mechanisms of bone remodelling. Front Biosci (Elite Ed). 2012; 4:2302–21. [PubMed: 22202038]

42. Crowe MJ, Doetschman T, Greenhalgh DG. Delayed wound healing in immunodeficient TGF-beta 1 knockout mice. J Invest Dermatol. 2000; 115(1):3–11. [PubMed: 10886500]

43. Schmid P, Cox D, Bilbe G, et al. TGF-beta s and TGF-beta type II receptor in human epidermis: differential expression in acute and chronic skin wounds. J Pathol. 1993; 171(3):191–7. [PubMed: 8277368]

44. Cowin AJ, Hatzirodos N, Holding CA, et al. Effect of healing on the expression of transforming growth factor beta(s) and their receptors in chronic venous leg ulcers. J Invest Dermatol. 2001; 117(5):1282–9. [PubMed: 11710945]

45. Jude EB, Blakytny R, Bulmer J, Boulton AJ, Ferguson MW. Transforming growth factor-beta 1, 2, 3 and receptor type I and II in diabetic foot ulcers. Diabet Med. 2002; 19(6):440–7. [PubMed: 12060054]

46. Wehrhan F, Hyckel P, Guentsch A, et al. Bisphosphonate-associated osteonecrosis of the jaw is linked to suppressed TGFbeta1-signaling and increased Galectin-3 expression: a histological study on biopsies. J Transl Med. 2011; 9:102. [PubMed: 21726429]

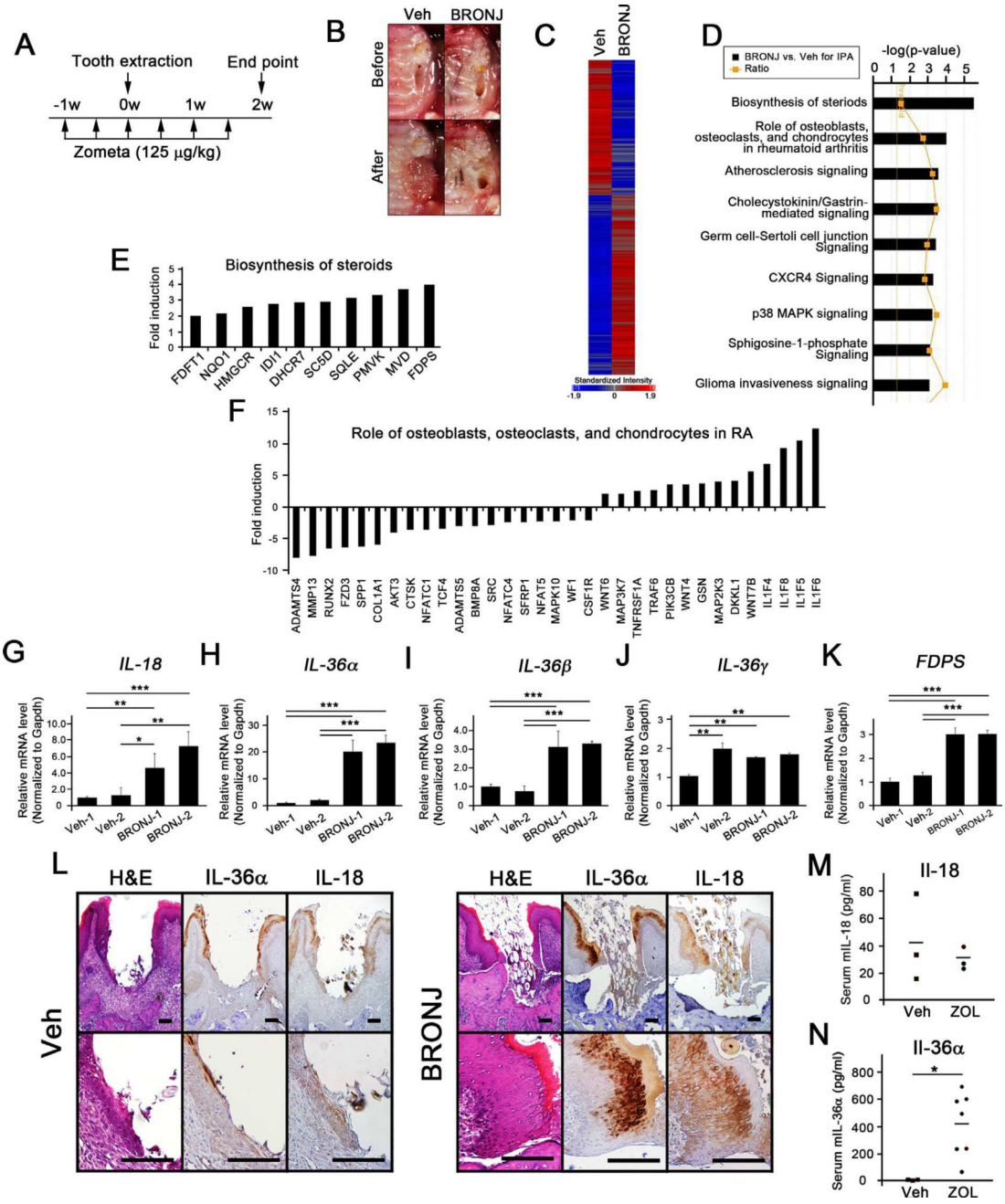

Fig. 1.

Microarray gene profiling identifies overexpressed IL-36 family members in ONJ-like lesions in mice. (*A*) A graphic representation of timeline used in this study. (*B*) Clinical illustration of the osteomucosal tissues before and after removal at the tooth-extracted areas photographed 2 weeks after tooth extraction. (*C*) A graphic representation of the microarray profiling that are differentially expressed more than fivefold were represented ($n = 3$ per group). (*D*) The ingenuity pathway analysis (IPA) of functional pathways that are associated with ONJ lesions. (*E*) Lists of genes involved in biosynthesis of steroids. (*F*) List of genes involved in role of osteoblasts, osteoclasts, and chondrocytes in rheumatoid arthritis. The

unhealed osteomucosal tissues at the tooth-extracted sites were harvested and subjected mRNA isolation, cDNA synthesis, and qRT-PCR for (*G*) IL-18, (*H*) IL-36α, (I) IL-36β, (*J*) IL-36γ, and (*K*) FDPS. The results are from two independent non-BRONJ and BRONJ lesions. (*L*) Staining for H&E and IHC staining for IL-36α at the tooth-extracted sites in vehicle (Veh)- or Zometa (ZOL)-treated mice. Scale bar = 100 μm. ELISA for (*M*) IL-18 and (*N*) IL-36α from the serum obtained from Veh- or ZOL-treated mice 2 weeks after tooth extraction. *$p<0.05$; **$p<0.01$; ***$p<0.001$. Results represent the means ± SD performed in triplicate unless otherwise indicated.

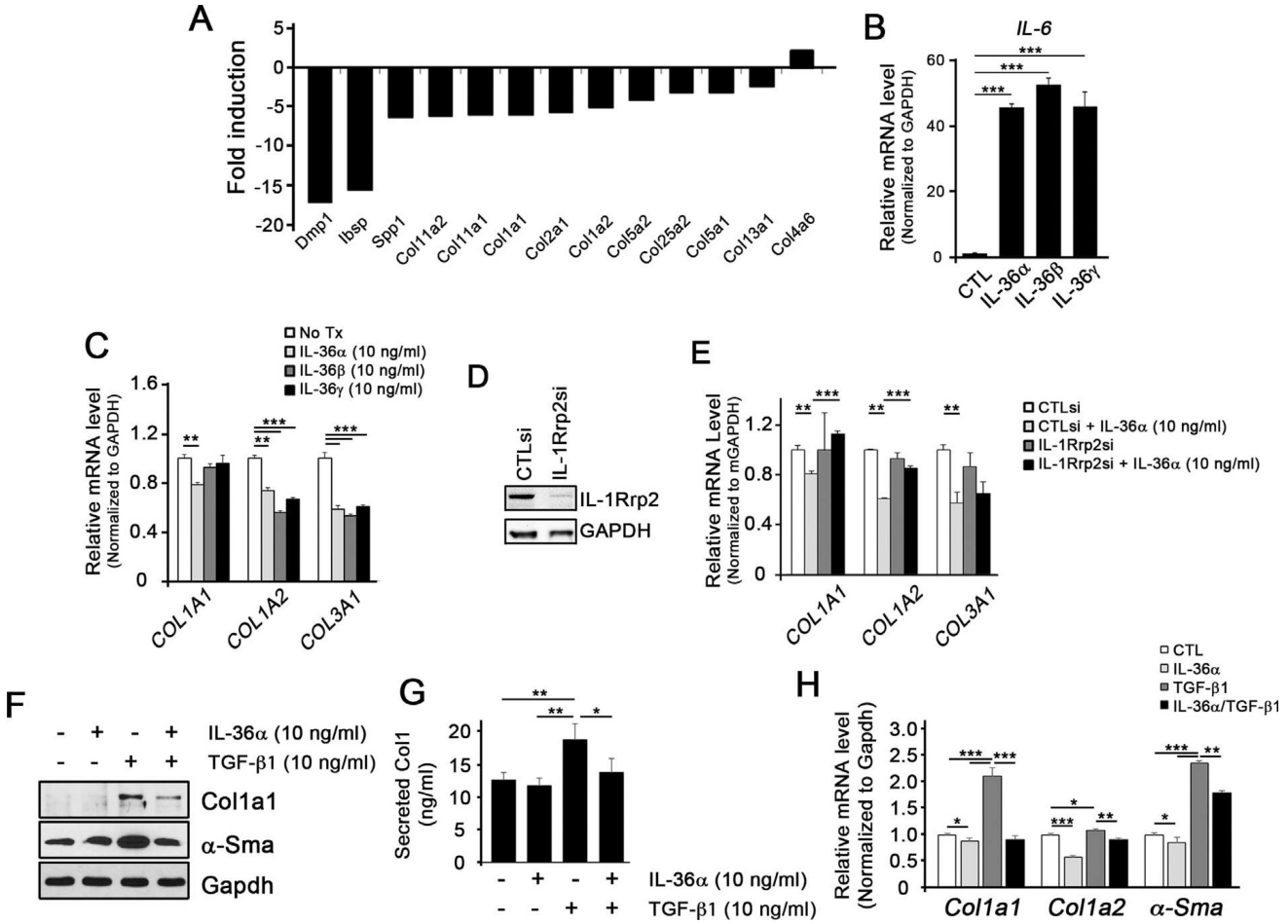

Fig. 2.

IL-36α inhibits expression of collagen and α-Sma in GMSCs. (*A*) List of genes associated with connective tissues (eg, collagenous and non-collagenous proteins) from the microarray data. (*B*) qRT-PCR of *Il-6* in gingival mesenchymal stem cells (GMSCs) treated with recombinant IL-36α, IL-36β, and IL-36γ for 4 days. (*C*) qRT-PCR of *Col1a1*, *Col1a2*, and *Col3a1* in GMSCs treated with recombinant IL-36α, IL-36β, and IL-36γ for 4 days. (*D*) Western blotting of IL-1Rrp2 after knocking down with control siRNA (CTLsi) or IL-1Rrp2 siRNA (IL-1Rrp2si) in GMSCs. (*E*) qRT-PCR of *Col1a1*, *Col1a2*, and *Col3a1* in GMSCs with IL-1Rrp2 knockdown and IL-36a treatment. (*F*) Western blotting of Col1a1 and α-Sma in GMSCs treated with IL-36α and TGF-β1 for 2 days. (*G*) ELISA for collagen type I from supernatants obtained from GMSCs treated with IL-36α and TGF-β1. (*H*) qRT-PCR of *Col1a1*, *Col1a2*, and *α-Sma* in GMSCs treated with recombinant IL-36α and TGF-β1 for 2 days. *$p<0.05$; **$p<0.01$; ***$p<0.001$. Results represent the means ± SD performed in triplicate.

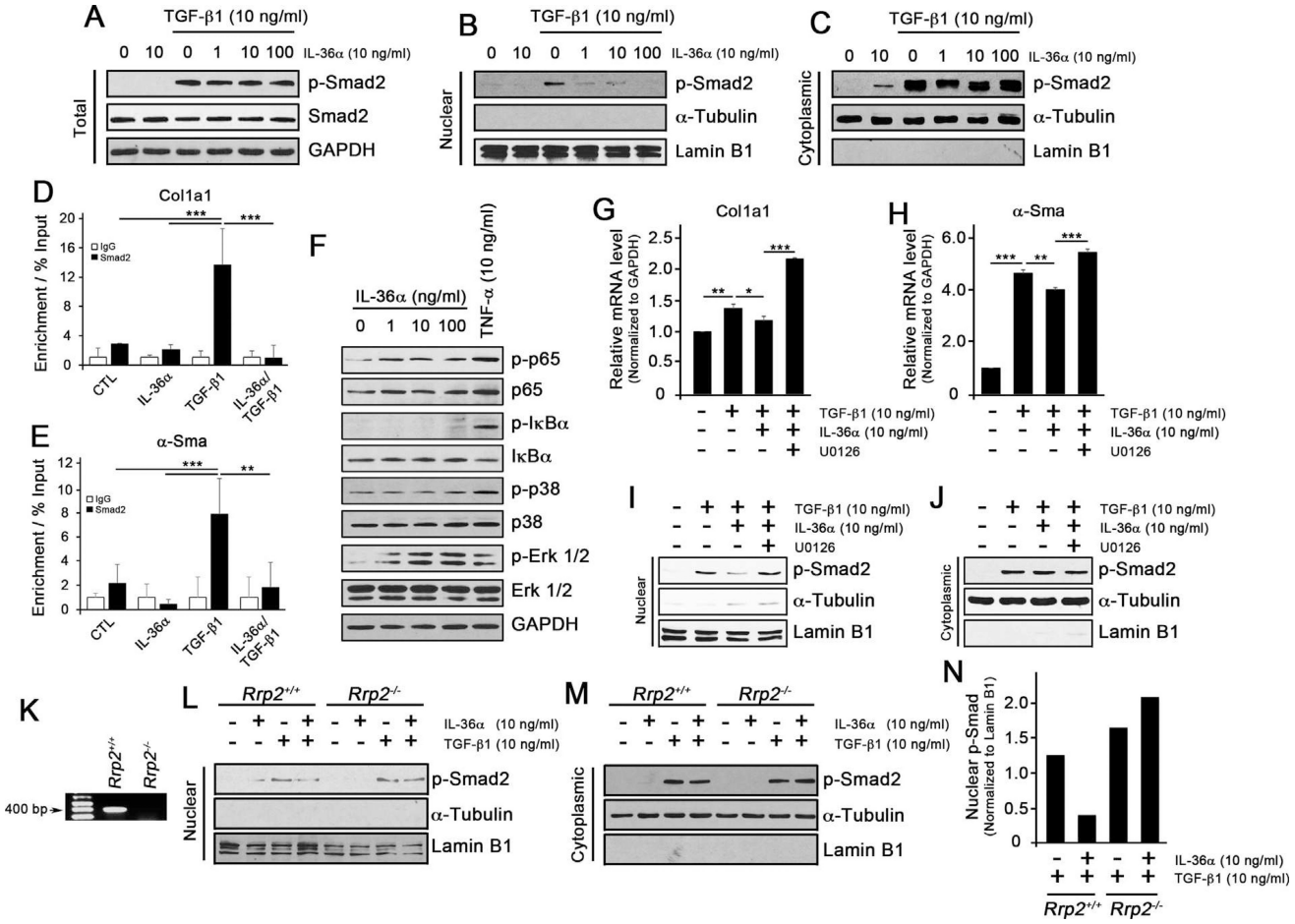

Fig. 3.

IL-36α inhibits nuclear translocation of activated Smad complex upon TGF-β1 treatment by activating the Erk signaling pathway. (*A*, *C*) Western blotting for p-Smad2 and Smad2 from the whole cell lysates, the nuclear extracts, and the cytoplasmic extracts in GMSCs treated with IL-36α for 6 hours and TGF-β1 for 2 hours. (*D*, *E*) Chromatin immunoprecipitation (ChIP) assay using IgG or Smad2 antibody followed by qRT-PCR using primers specific to the promoter regions of *Col1a1* and *α-Sma*. The values were normalized to the internal control. (*F*) Western blotting for indicated antibodies in GMSCs treated with IL-36α or TNF-α for 6 hours. (*G*, *H*) qRT-PCR analysis for *Col1a1* and *α-Sma* in GMSCs treated with U0126 (10 μM) and IL-36α (10 ng/mL) for 6 hours before adding TGF-β1 (10 ng/mL). Cells were harvested after 2 days. (*I*, *J*) Western blotting against p-Smad2 and Smad2 from the nuclear and cytoplasmic extracts. (*K*) PCR for genomic *IL-1Rrp2* in GMSCs obtained from *IL-1Rrp2*$^{+/+}$ or *IL-1Rrp2*$^{-/-}$ mice. (*L*, *M*) Western blotting for p-Smad2 from the nuclear and cytoplasmic extracts in *IL-1Rrp2*$^{+/+}$ or *IL-1Rrp2*$^{-/-}$ GMSCs treated with IL-36α for 6 hours followed by TGF-β1 for 2 hours. (*N*) Quantification of the Western blotting (*L*) of p-Smad2 normalized to the Lamin B1 using ImageJ. *p<0.05; **p<0.01; ***p< 0.001. Results represent the means ± SD performed in triplicate.

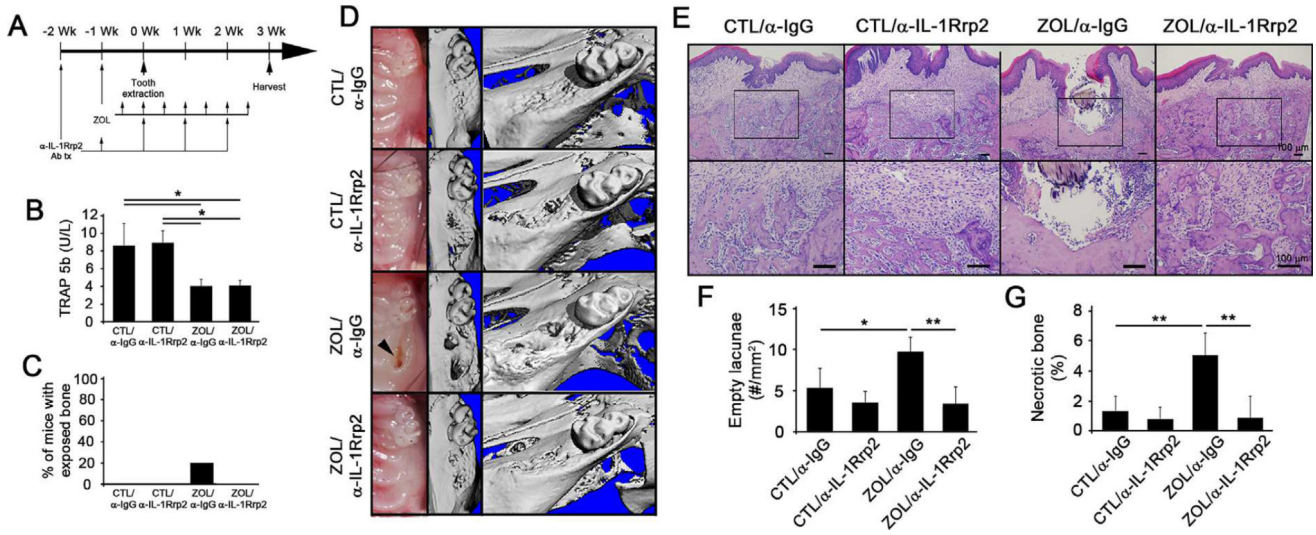

Fig. 4.

Anti-IL-1Rrp2 neutralizing antibody rescues ONJ lesions in mice. (*A*) A graphic representation of the timeline used in this study. (*B*) ELISA for TRAP 5b from the serum obtained from mice at the end of the experiments. (*C*) Percent of mice with exposed bone was assessed (n = 8–10 per group). (*D*) Clinical illustrations of the osteomucosal tissues at the tooth-extracted areas (left panels) and μCT scans of the maxillae taken from the occlusal views (middle panels) and the angled views (right panels). (*E*) H&E-stained tissues at tooth-extracted sites. Scale bar = 100 μm. (*F, G*) The numbers of empty lacunae per mm^2 and the percentage of necrotic bones were quantified. *p<0.05; **p<0.01; ***p< 0.001.

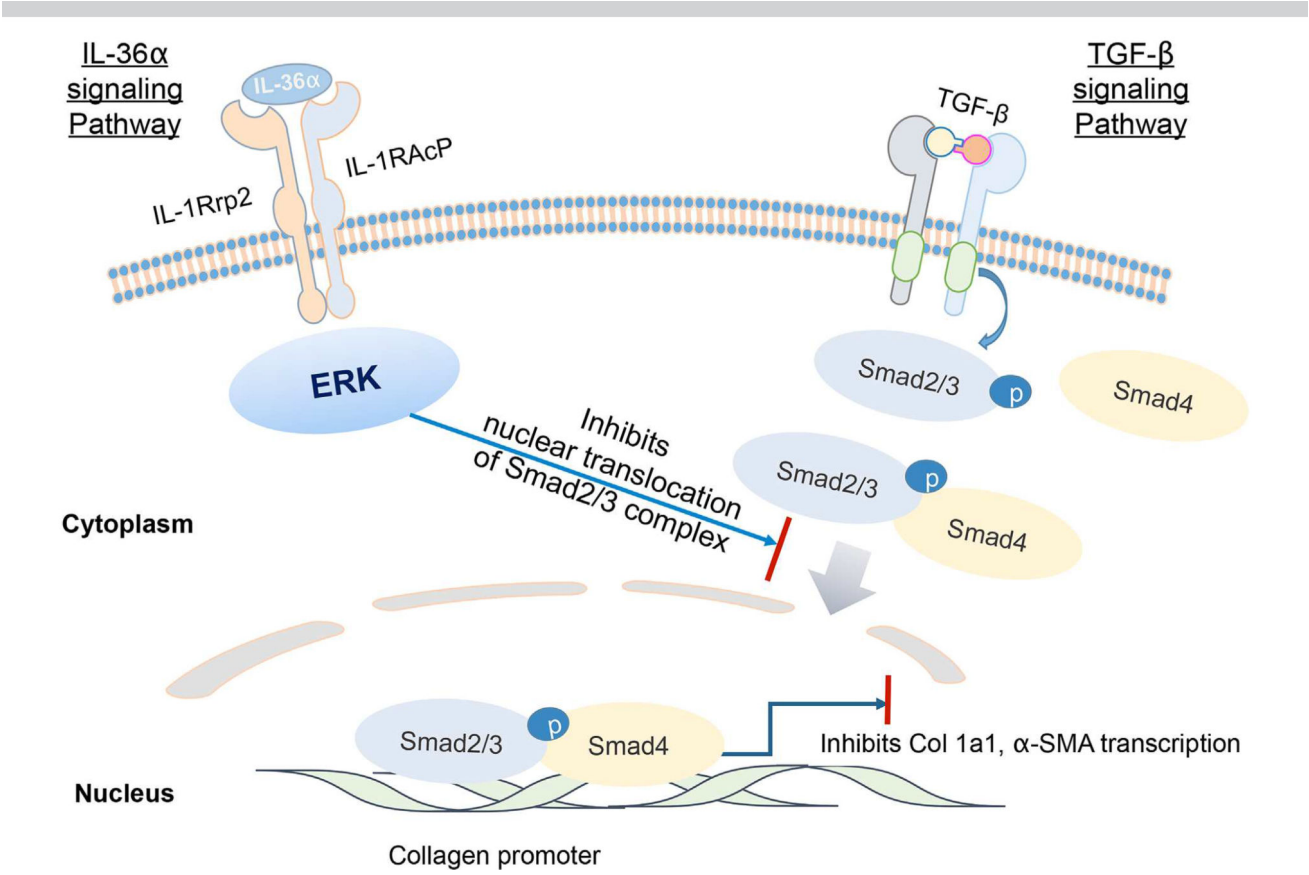

Fig. 5.

Proposed model. TGF-β1 binds TGF-β receptor and causes phosphorylation of Smad2/3, which in turns translocates into the nucleus and activates the target genes such as *Col1a1* or *α-Sma*. IL-36α binds to IL-36 receptor complex and activates the ERK signaling pathway. Activated Erk inhibits translocation of TGF-β1-activated Smad complex, thereby suppressing the Smad-mediated activation of gene expression.